

# An automated procedure for estimating the leaf area index (LAI) of woodland ecosystems using digital imagery, MATLAB programming and its application to an examination of the relationship between remotely sensed and field measurements of LAI

Sigfredo Fuentes<sup>A,B,C</sup>, Anthony R. Palmer<sup>B</sup>, Daniel Taylor<sup>B</sup>, Melanie Zeppel<sup>B</sup>, Rhys Whitley<sup>B</sup> and Derek Eamus<sup>B</sup>

<sup>A</sup>Plant Research Centre, University of Adelaide, Waite Campus, PMB 1 Glen Osmond, SA 5064, Australia.

<sup>B</sup>Institute for Water and Environmental Resource Management (IWERM), University of Technology, Sydney, NSW 2007, Australia.

<sup>C</sup>Corresponding author. Email: sigfredo.fuentes@adelaide.edu.au

*This paper originates from a presentation at the 5th International Workshop on Functional–Structural Plant Models, Napier, New Zealand, November 2007.*

**Abstract.** Leaf area index (LAI) is one of the most important variables required for modelling growth and water use of forests. Functional–structural plant models use these models to represent physiological processes in 3-D tree representations. Accuracy of these models depends on accurate estimation of LAI at tree and stand scales for validation purposes. A recent method to estimate LAI from digital images ( $LAI_D$ ) uses digital image capture and gap fraction analysis (Macfarlane *et al.* 2007b) of upward-looking digital photographs to capture canopy  $LAI_D$  (cover photography). After implementing this technique in Australian evergreen *Eucalyptus* woodland, we have improved the method of image analysis and replaced the time consuming manual technique with an automated procedure using a script written in MATLAB 7.4 ( $LAI_M$ ). Furthermore, we used this method to compare MODIS LAI values with  $LAI_D$  values for a range of woodlands in Australia to obtain LAI at the forest scale. Results showed that the MATLAB script developed was able to successfully automate gap analysis to obtain  $LAI_M$ . Good relationships were achieved when comparing averaged  $LAI_D$  and  $LAI_M$  ( $LAI_M = 1.009 - 0.0066 \cdot LAI_D; R^2 = 0.90$ ) and at the forest scale, MODIS LAI compared well with  $LAI_D$  ( $MODIS \text{ LAI} = 0.9591 \cdot LAI_D - 0.2371; R^2 = 0.89$ ). This comparison improved when correcting  $LAI_D$  with the clumping index to obtain effective LAI ( $MODIS \text{ LAI} = 1.0296 \cdot LAI_e + 0.3468; R^2 = 0.91$ ). Furthermore, the script developed incorporates a function to connect directly a digital camera, or high resolution webcam, from a laptop to obtain cover photographs and LAI analysis in real time. The later is a novel feature which is not available on commercial LAI analysis softwares for cover photography. This script is available for interested researchers.

**Additional keywords:** digital imagery, *Eucalyptus*, leaf area index, MATLAB, MODIS LAI, remote sensing.

## Introduction

Leaf area index (LAI) can be defined as the total one-sided area of leaf tissue per unit ground surface area (Watson 1947). LAI is an important parameter used to validate plant architectural models (De Reffye *et al.* 1995). Accurate estimates of LAI are also important for functional–structural plant models, since leaf area strongly influences rates of evapotranspiration and photosynthesis of trees (Nemani *et al.* 1993; Villalobos *et al.* 1995). Consequently, estimation of this parameter is also important for modelling forest growth and water use (Macfarlane *et al.* 2007b), as it determines the productivity and physical and biophysical interactions between land surfaces and the atmosphere (Chen and Cihlar 1995). Finally, accurate estimations of LAI are critical to scale-up leaf-based

physiological measurements to the whole tree (Ewert 2004), tree-based measurements (e.g. sap flow) to the stand scale (Zeppel *et al.* 2004, 2008; Whitley *et al.* 2008) and to scale from regional to continental processes of land surface-atmosphere exchange (Lu and Shuttleworth 2002; Ewert 2004). LAI can be directly measured using destructive methods or indirectly estimated.

### Direct v. indirect LAI measurement

Direct measurements of LAI (allometry or litterfall) are difficult and time consuming to perform on trees (Cutini *et al.* 1998). Furthermore, these methods do not easily allow a representative spatial and temporal resolution of LAI at the forest stand scale (Chason *et al.* 1991). Consequently, ground-based indirect methods have been developed and are more commonly used to

estimate LAI. Typically these are based on measurements of radiation transmission through the canopy (Bréda 2003), for example the Li-Cor-2000 (Plant canopy analyser; Li-Cor, Lincoln, NE, USA) (Villalobos *et al.* 1995; Cutini *et al.* 1998; Bréda 2003; Arias *et al.* 2007). However, the cost of the Li-Cor-2000 can be prohibitive (Macfarlane *et al.* 2007b) and these units can underestimate LAI between 10–40% (Macfarlane *et al.* 2000) in forests. Other indirect methods have been developed using digital photography.

#### *Fisheye v. cover digital photography*

Fisheye photography or hemispherical methods have been proposed as a less costly alternative, which measures the gap fraction at more than one zenith angle. However, the downside of these techniques is that, in reality, estimates of the light extinction coefficient ( $k$ ) are usually flawed owing to foliage clumping, inaccurate gap fraction retrieval and woody area. An improved fisheye technique can be achieved using ‘fullframe fisheye photography’, which increases the resolution and accuracy of gap fraction retrieval (Macfarlane *et al.* 2007a). Most recently, estimation of LAI indirectly using digital or cover photography and gap fraction analysis have been developed and this provides an accurate and rapid estimation of LAI (Macfarlane *et al.* 2007b). Furthermore, studies comparing hemispherical, fullframe fisheye and cover photography (digital) have concluded that the later is the best option for routine, indirect measurements and monitoring of LAI in broadleaf forests (Macfarlane *et al.* 2007b). Moreover, the cover photography method outperforms fisheye photography, since the former can be applied during daylight hours, are of much higher resolution (less sensitive to photographic exposure), sky luminance is more even and the narrow viewing angle was better suited to small rectangular plots. However, the disadvantage is that the cover photography method could not be automated using analysis softwares available (Macfarlane *et al.* 2007a, 2007b, 2007c).

#### *Commercially available softwares for LAI analysis*

The hemispherical or fullframe fisheye photography techniques require complicated analysis and specialised software (Frazer *et al.* 2001; Bréda 2003; Macfarlane *et al.* 2007a, 2007b). The majority of these softwares are commercially available (some are freeware: *F*) to researchers, such as: Hemiview, Hemiphot, GLA, DHP-TRACWin, CANEYE (*F*) and WinSCANOPY (Regent Instruments, Ste-Foy, Quebec, CA). These softwares were mainly developed to analyse hemispherical photography and fullframe fish eye photography (Macfarlane *et al.* 2007b). On the contrary, the cover photography method uses normal digital cameras and upward-looking digital photographs to capture canopy LAI ( $\text{LAI}_D$ ) and analyses these images at a single zenith angle (0–15°), using commercial image processing software (Photoshop 7.0; Adobe Systems Inc., San Jose, CA, USA). This process is time consuming (5 min per image) and, hence, costly when analysing 50 or more images for a single site. With the improved availability of cost effective high resolution digital cameras there is an incentive to further automate this technique. Recently, WinSCANOPY have incorporated analysis of cover photography, which is not fully automated. A comparison between WinSCANOPY and the method using Adobe

Photoshop 7.0 ( $\text{LAI}_D$ , which is used as a baseline in this study) was tested by Macfarlane *et al.* (2007c). This study found that results between WinSCANOPY and Photoshop have little difference in LAI estimation; however, they varied from individual images, as evidenced by the small correlation coefficients between the two methods for crown porosity and the clumping index (Macfarlane *et al.* 2007b). The availability of a tool to automate analysis of LAI digital pictures will allow a rapid method to up-scale this parameter to broader scales and to calibrate LAI obtained from satellite imagery, such as MODIS LAI.

#### *MODIS-LAI estimates*

At the forest and catchment scale, LAI estimates can be derived from satellite spectral reflectance measurements (Nemani *et al.* 1993). This method is based on either the strong relationship between LAI and NIR/RED ratio (Peterson *et al.* 1987; Carlson and Ripley 1997) or the normalised difference vegetation index (NDVI). High correlations between NDVI and LAI have been found for non-continuous herbaceous crops, such as grapevines (Johnson 2003) and forests (Peterson *et al.* 1987; Lu and Shuttleworth 2002). MODIS LAI uses radiative transfer (RT) simulations, which simulates average over satellite pixel RT field, such as Moderate resolution Imaging Spectroradiometer (MODIS) LAI algorithm (Huang *et al.* 2008). The MODIS 8-day 1 km LAI/FPAR product 4 (MOD15A2 C4) (Knyazikhin *et al.* 1998) is an improvement on the simple band ratio products and was available for the study period from the NASA Distributed Active Archive Centre. Currently, collection 5 (C5) has been released, which increases amount of best quality retrievals over broad leaf forests. A suitable ground-based LAI measurement is necessary to validate and assess uncertainties associated with satellite-derived products such as MODIS LAI (Tian *et al.* 2002).

In this paper, we describe an image analysis tool written in MATLAB 7.4 and compare results using this tool ( $\text{LAI}_M$ ) with  $\text{LAI}_D$ . The tool developed is able to batch-process digital images using gap fraction analysis, making the procedure automatic (on clear or fully overcast day images) or semi-automatic (on patchy cloudy day images). We also compared  $\text{LAI}_D$  with MODIS LAI values for a range of woodlands in New South Wales (NSW) and Western Australia (WA) to validate MODIS LAI data at the forest scale. Since digital images and analysis includes trunks and brunches, it is argued that estimates correspond to Plant Area Indices (PAI) rather than LAI (Bréda 2003). However, to maintain a consistent nomenclature we will use LAI for  $\text{LAI}_D$ ,  $\text{LAI}_M$  and MODIS LAI in results.

## **Materials and methods**

#### *Site locations*

Data included in this study were obtained from sites described in Table 1.

#### *Digital image acquisition*

A Nikon (Tokyo, Japan) Coolpix 995 (3 145 728 pixels in total) mounted on a tripod with a bubble level to obtain images at the zenith angle was used to acquire digital images from all sites. Images were collected at 1.5 m from the ground as FINE JPEG. The camera was set to automatic exposure using

**Table 1.** Sites of 1 ha approximately in New South Wales and Western Australia, Australia, were used to validate the script developed (\*) and MODIS LAI results (all sites)

Site name	Location	State
Castlereagh*	33°39'41.54"S; 150°46'58.27"E	NSW
Bago*	35°39'20.6"S; 148°09'07.5"E	NSW
Paringa*	31°25'16.7"S; 150°36'28"E	NSW
Sunnycorner*	33°23'36.63"S; 149°52'44.47"E	NSW
Hornsby*	33°40'3"S; 151°10'32"E	NSW
Condobolin	33°3'12.40"S; 146°6'53.79"E	NSW
Quairadlin	32°46'18.82"S; 117°6'26.48"E	WA
Wandoor NP	32°45'0.02"S; 116°55'42.00"E	WA

F2 lens, which gives a zoom angle of ~35° across the diagonal, or ~0–15° zenith angle range. In all sites, five images every 10 m were taken over five linear transect located 10 m apart. This procedure was repeated twice per site, giving a total of 50 images per site. Images were collected in August 2006 at all sites.

#### MATLAB script development

We used MATLAB 7.4 (The Mathworks Inc., Natick, MA, USA) and the Image Processing Toolbox to generate a script to batch process numerous upward-looking digital images (at least 50 per site). The objective was to automate the estimation of LAI from five different woodland sites within NSW (Table 1) and to compare results of LAI<sub>M</sub> with LAI<sub>D</sub> and MODIS LAI. The user inputs answers to seven questions (Table 2) made by the script at the start of each batch process.

#### Filtering clouds from images

A binary (black and white) image was required to simplify gap fraction analysis. However, when trying to convert an RGB (red–green–blue) patchy cloud sky image (Fig. 1a) to a binary image (Fig. 1b) without filtering it tends to include clouds as leaf cover, leading to overestimations of LAI<sub>M</sub>. To overcome this, the image colour and brightness components where analysed separately: Figs 2a (blue), 2b (green), 2c (red), 2d (hue), 2e (saturation) and 2f

**Table 2.** Questions from the script developed to be answered by the user at the beginning of the analysis

Question	Script outputs	User input
a	Name of files	Alphanumeric
b	Initial image	Numeric (1 – n)
c	Last image	Numeric (1 – n)
d	Number of subdivisions	Numeric (1 – n)
e	Gap fraction threshold	Numeric (0 – 1)
f	Light extinction coefficient	Numeric (0 – 1)
g	Number of approximations	Numeric (1 – n)

(intensity). The best cloud filters where the blue (Fig. 2a) and intensity (Fig. 2f) components, since they gave the best contrast between foliage cover and sky plus clouds.

#### Selecting luminance threshold

The blue band (450–495 nm) of each image was extracted as a histogram and explored to identify a suitable threshold between foliage and sky (Fig. 3). In this procedure, the selection of a suitable luminance value threshold (T) from the blue band histograms can be fully automated for numerous images (for clear or completely overcast days) or manually generated for each image (for patchy cloud days). After assigning a suitable T (cursor selection), the image is transformed into a binary image for gap analysis. In the program, there is an option (Question g) to give the user several attempts (1 – n) to select an accurate luminance threshold from the blue image component. This is done by viewing the original RGB image and the binary image side by side (Fig. 1) to see whether small gaps were missed or considered in filtered binary image. This feature, which helps to avoid over- or under-estimates of LAI<sub>M</sub>, is not readily available in Photoshop 7.0 or commercial softwares, such as WinSCANOPY.

#### Images gap analysis

The script developed performs gap analysis by automatically dividing each binary image into several sub-images defined by the user (Question d). From each subimage, the program counts



**Fig. 1.** (a) Typical upward looking digital image in a patchy cloudy day. (b) Filtered binary image to avoid cloud inclusion in LAI<sub>M</sub> analysis. Gap analysis considering nine image subdivisions at question d=3 (3 × 3 or n=9).

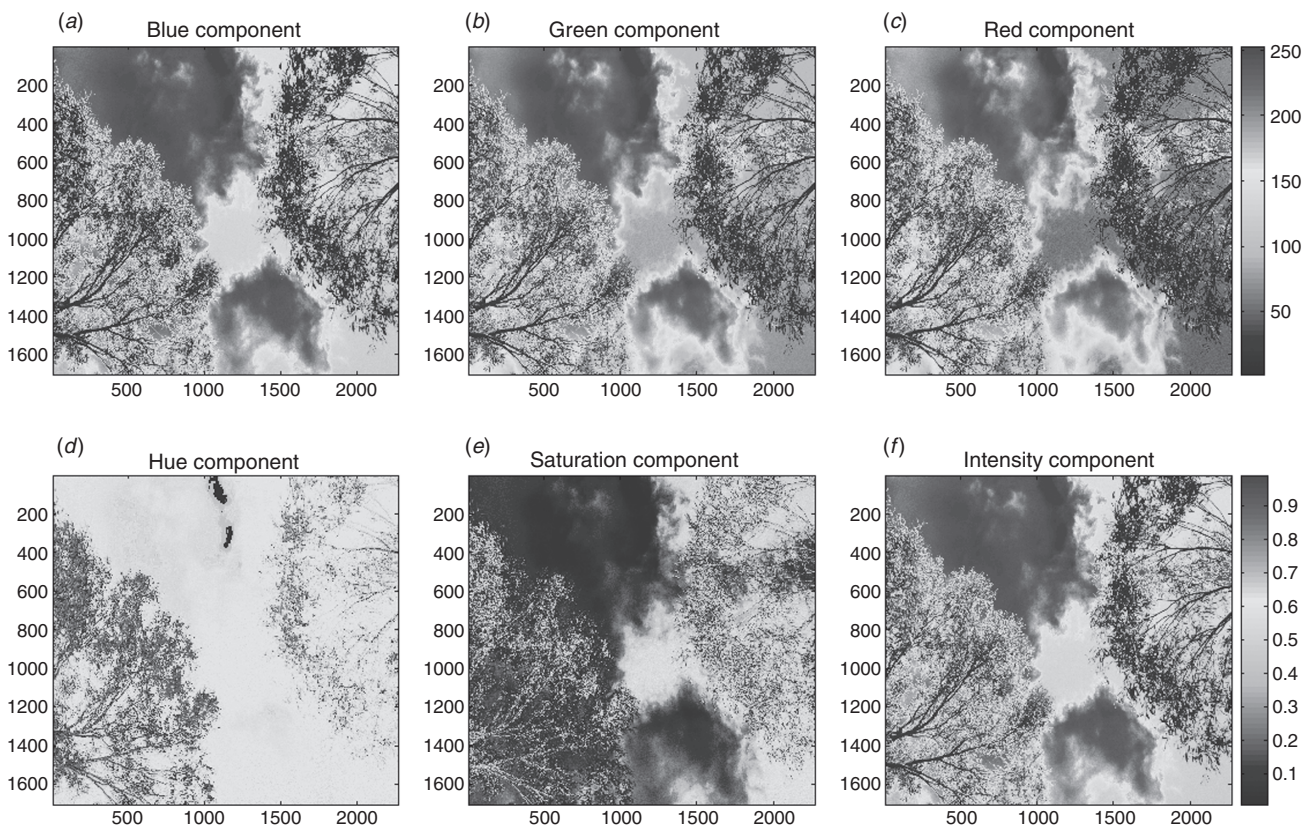


**Fig. 2.** Image components separation using MATLAB to obtain a cloud filtering rule for the script written in MATLAB. (a) Blue and (f) intensity components were best suited for cloud filtering.

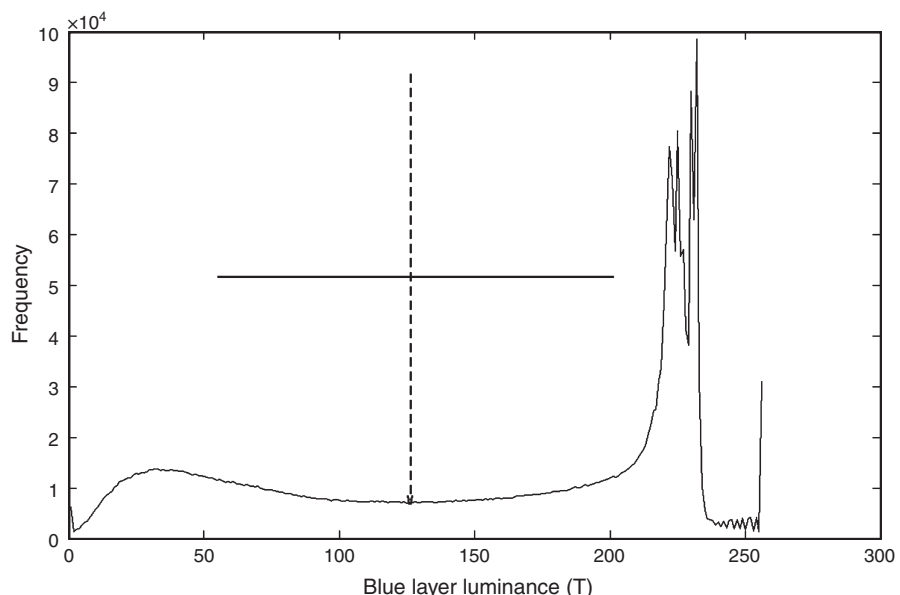


**Fig. 3.** Luminance distribution for a single image showed as a blue component histogram generated by the script developed in MATLAB. Sky and canopy luminance peaks can be seen at the left and right sides of the graph, respectively. A suitable threshold for clouds exclusion can be achieved in the middle, around lowest value. Cross cursor is a selector generated by the script for easy threshold selection.

the total of pixels corresponding to sky (S) and leaves (L). A big gap is considered when the ratio S/L in each sub-image is larger than a user-specified value (Question e). When this occurs, the pixel count for S is added to the big gap count for that particular full image. If the ratio observed is smaller than the user-specified value for a specific sub-image, the pixel count contribution to the total big gap count of that particular image is equal to zero. A sensitivity test was performed using 10 random images per site and subdividing each image by  $3 \times 3$  ( $n=9$ );  $4 \times 4$  ( $n=16$ );  $5 \times 5$  ( $n=25$ ) and  $6 \times 6$  ( $n=36$ ). No significant differences were seen in the LAI<sub>M</sub> obtained at different subdivisions (data not shown). Therefore, it was decided to divide all images at  $3 \times 3$  ( $n=9$ ) subdivisions to optimise data analysis time.

To analyse 50 images automatically, the script took approximately 10 minutes using an Apple Macbook Core Duo with 2.0 Gb. RAM at 2.3 Ghz. Individual image analysis timing depended of the number of approximations selected by the user. Considering this number as three, it takes 1 min approximately to analyse a single image. Also, a big gap threshold of 0.75 was the most appropriate for all images, since it gave the best comparison with LAI<sub>D</sub> (LAI<sub>D</sub> between 0.7–1.7).

The fractions of foliage projective cover ( $f_f$ ), crown cover ( $f_c$ ) and crown porosity ( $\Phi$ ) are calculated from Macfarlane *et al.* (2007b) as:

$$f_c = 1 - \frac{lg}{tp}, \quad (1)$$

$$f_f = 1 - \frac{tg}{tp}, \quad (2)$$

and

$$\Phi = \frac{f_f}{f_c}, \quad (3)$$

where lg is large gap pixels, tg is the total pixels in all gaps and tp is the total gap pixels. LAI<sub>M</sub> is calculated from Beer's Law, assuming an extinction co-efficient ( $k$ ) of 0.5, which is suitable for eucalypt trees (Macfarlane *et al.* 2007b), (this value can be altered in the script Question f):

$$LAI_M = -f_c \frac{\ln \Phi}{k}, \quad (4)$$

and the clumping index at the zenith,  $\Omega(0)$ , was calculated as follows:

$$\Omega(0) = \frac{(1 - \Phi) \ln(1 - f_f)}{\ln(\Phi)f_f}. \quad (5)$$

The clumping index is a correction factor to obtain effective LAI (LAI<sub>e</sub>), which is the product of:

$$LAI_e = LAI_M \times \Omega(0). \quad (6)$$

Eqn 5 describes the non-random distribution of canopy elements. If  $\Omega(0) = 1$ , means that the canopy displays random dispersion; for  $\Omega(0) >$  or  $< 1$ , the canopy is defined as clumped. LAI<sub>e</sub> was not considered for the script development and results presented in this paper; however, it is available to be calculated in the last version of the script.

After image analysis, the script stores all the calculated parameters (LAI<sub>M</sub>,  $f_f$ ,  $f_c$ ,  $\Phi$ ,  $\Omega(0)$  and LAI<sub>e</sub>) in a .txt file, which can be readily read by Excel. The same Eqns 1–6 were used to calculate LAI<sub>D</sub> using Adobe PhotoShop 7.0 and the methodology described by Macfarlane *et al.* (2007b).

#### *MODIS LAI analysis*

Following the capture of digital images and determination of LAI<sub>D</sub> for eight examples of *Eucalyptus* woodlands in NSW and WA (Table 1), we assessed the relationship between LAI<sub>D</sub> and MODIS LAI products for each of the ground measurements. We extracted the 8-day 1 km MODIS LAI data for NSW and WA from the MODIS distributed archive and imported these into a GIS software package (IDRISI; Clark Laboratories, Worcester, MA, USA) (Fig. 6a, b). The ground sampling sites were established along a precipitation gradient (450–1400 mm) in NSW and WA. 8-day MODIS LAI values for ground sampling stations (of ~1 ha) were extracted using a data-drill. At each ground sampling station, LAI<sub>D</sub> was calculated from at least 50 randomly collected images from the 1 ha stations within the 1 km MODIS pixel. Individual modelled MODIS LAI values for each sampling occasion were selected from the 8-day image closest to the date of the LAI<sub>D</sub> sampling event. Although seasonal variations in MODIS LAI was apparent at each sampling site (i.e. range from LAI 1 to 4 in wet sites), the ground sampling events coincided with periods when MODIS LAI closely approximated LAI<sub>D</sub>. The ground sampling excluded the contribution of understorey LAI, and was conducted during the dry season when the contribution of the understorey would have been at its minimum.

#### *Statistical analysis*

To compare the performance of the script developed (LAI<sub>M</sub>) and MODIS LAI with the baseline data (LAI<sub>D</sub>), linear regression analyses were done between LAI<sub>D</sub>; LAI<sub>e</sub> and LAI<sub>M</sub>; MODIS LAI. A sensitivity analysis of LAI<sub>M</sub> to T was conducted considering a variation of T of maximum  $\delta t = +20$  and minimum  $\delta t = -30$  (Fig. 8). Images taken on clear days conditions ( $n=50$ ) and on patchy cloudy day conditions ( $n=30$ ) were selected for the sensitivity analysis. Patchy cloudy days were avoided for data collection due to high variability in luminosity. Therefore, this explains the lower number of images on patchy cloudy days. The statistical analysis was done using MATLAB 7.14 and the curve fitting toolbox.

## **Results and discussion**

#### *LAI estimations using the script developed*

The automated procedure to analyse digital images using the script resulted in a good averaged LAI<sub>M</sub> compared with the averaged LAI<sub>D</sub> for five sites (Fig. 4, open circles) (LAI<sub>M</sub> = 1.009–0.0066 LAI<sub>D</sub>; R<sup>2</sup> = 0.90). Standard errors were also similar between LAI<sub>D</sub> and LAI<sub>M</sub>. When patchy clouds were present in the images, the manually generated threshold was more appropriate to obtain accurate individual LAI<sub>M</sub> from single images when compared with LAI<sub>D</sub> (i.e. LAI<sub>M</sub> = 0.95 LAI<sub>D</sub>; R<sup>2</sup> = 0.95, from 50 images; Hornsby site, data not shown). All the sites showed mostly clumped canopies (at different levels) as can

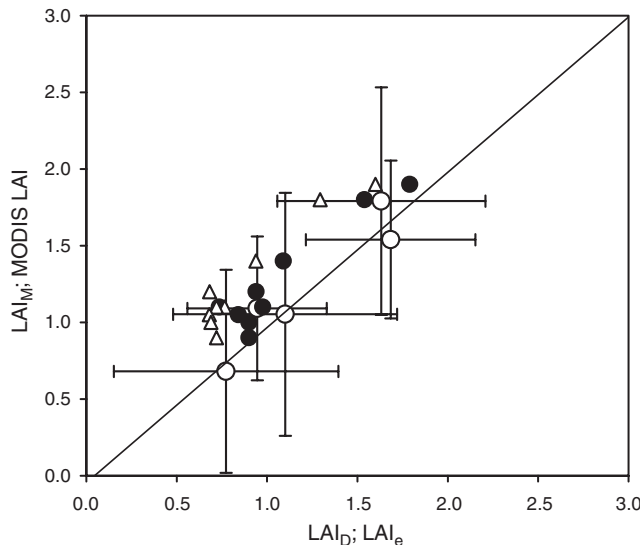


**Fig. 4.** Comparison between  $\text{LAI}_M$  and  $\text{LAI}_D$  (open circles) for five sites in NSW; MODIS LAI and  $\text{LAI}_D$  (closed circles) and MODIS LAI and  $\text{LAI}_e$  (open triangles) for eight woodland sites in NSW and WA, Australia. Standard error bars for  $\text{LAI}_D$  v.  $\text{LAI}_M$  data and the 1:1 line are shown in the graph.

be seen in Fig. 5 [ $\Omega(0) < 1$ ], with averaged minimum values of 0.6 for Castlereagh and maximum of 0.84 for Bago. The averaged  $\Omega(0)$  considering all sites was 0.78. This makes clear that corrections using the clumping index (using Eqn 6) need to be introduced in the calculation of  $\text{LAI}_M$  and  $\text{LAI}_D$  to obtain  $\text{LAI}_e$ .

According to Bréda (2003), PAI rather than LAI terminology should be used for techniques using digital photography, since woody area (trunks and branches) is included in the analysis contributing to overestimations of LAI. However, the largest woody contributions in  $\text{LAI}_D$  (overestimations) are associated to images close to the main stem of tall trees. In contrast, using this technique in woodlands where species with lightly coloured trunks [e.g. ghost gums (*Eucalyptus papuana*)] are mostly

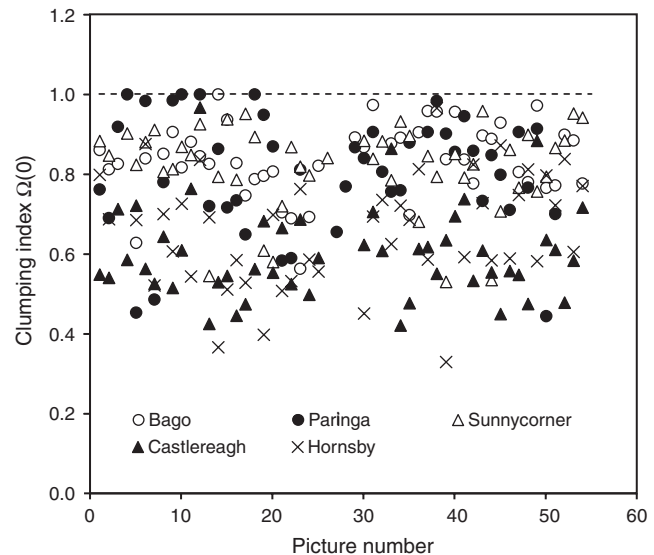


**Fig. 5.** Calculated clumping index [ $\Omega(0)$ ] using Eqs 2, 3 and 5 for individual images taken at five sites in NSW, Australia ( $n=268$ ).

present, could contribute to under-estimations of  $\text{LAI}_D$ , since these stems can be mistaken for sky in the script filtering method if the fully automated routine proposed in this paper is used. Using the manual technique can remove this source of error. Alternatively, images can be taken a couple of metres away from such stems to minimise woody inclusion and avoiding times of the day when trunks or branches receive direct sunlight. Finally, corrections for woody area are considered smaller for the digital image technique, than hemispherical photography (wide angle:  $0-57^\circ$ ), since the narrow angle of digital images ( $0-15^\circ$ ) reduces inclusion of stems and therefore their contribution to  $\text{LAI}_D$  (Kucharik *et al.* 1997).

The choice of a suitable T value, within the blue component of a image, is also critical to avoid over- or under-estimations of  $\text{LAI}_D$  (Macfarlane *et al.* 2007b). Therefore, the image comparison

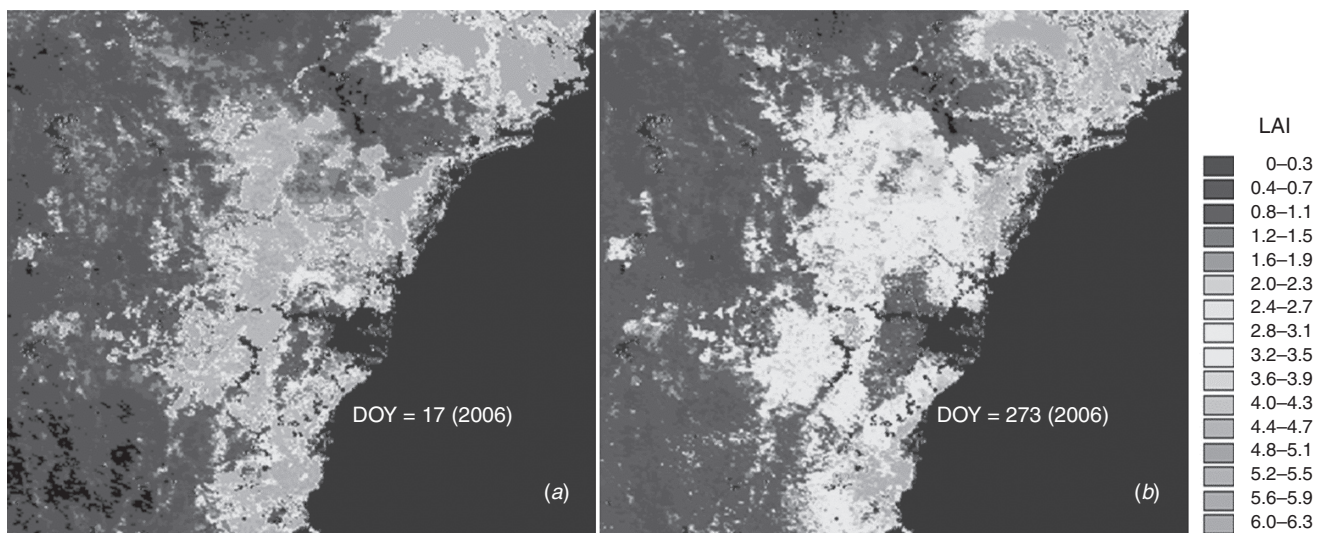


**Fig. 6.** MODIS LAI data combined with GIS (IDRISI) for summer (a) and spring (b) in NSW, Australia 2006.

tool available within the script (Fig. 1*a, b*) is very useful to avoid errors in the LAI<sub>D</sub> calculation. Suitable T values are very similar within images taken on clear or completely overcast days (Fig. 7*a*). An individual analysis of 2–5 images will be enough to obtain a common threshold for batch-analysis of images taken on these weather conditions. The other critical factors for LAI<sub>D</sub> calculations are crown cover ( $f_c$ ) and porosity ( $\Phi$ ), which are highly dependant of the visual selection of large, between-crowns gaps. Using the script developed, the operator subjectivity can be avoided, when selecting large gaps through calibration of sub-image size and gap fraction ratio for different types of woodlands. This calibration is readily available for the script from other studies using digital

photography compared with allometric measurements. Therefore, one of the most important advantages of the methodology described here is that images can be analysed using different gap and image analysis techniques. This is in contrast to most commercial ground-based LAI analysers (such as Li-Cor 2000) which only provide the processed output and not the unprocessed data.

A useful feature of the script was also developed to acquire images using a high resolution web-cam attached to a laptop for in-field real-time digital image acquisition and analysis described in this paper. This feature is not available on commercial softwares to analyse cover photography (Adobe Photoshop 7.0 and WinSCANOPY). The script developed in this study is

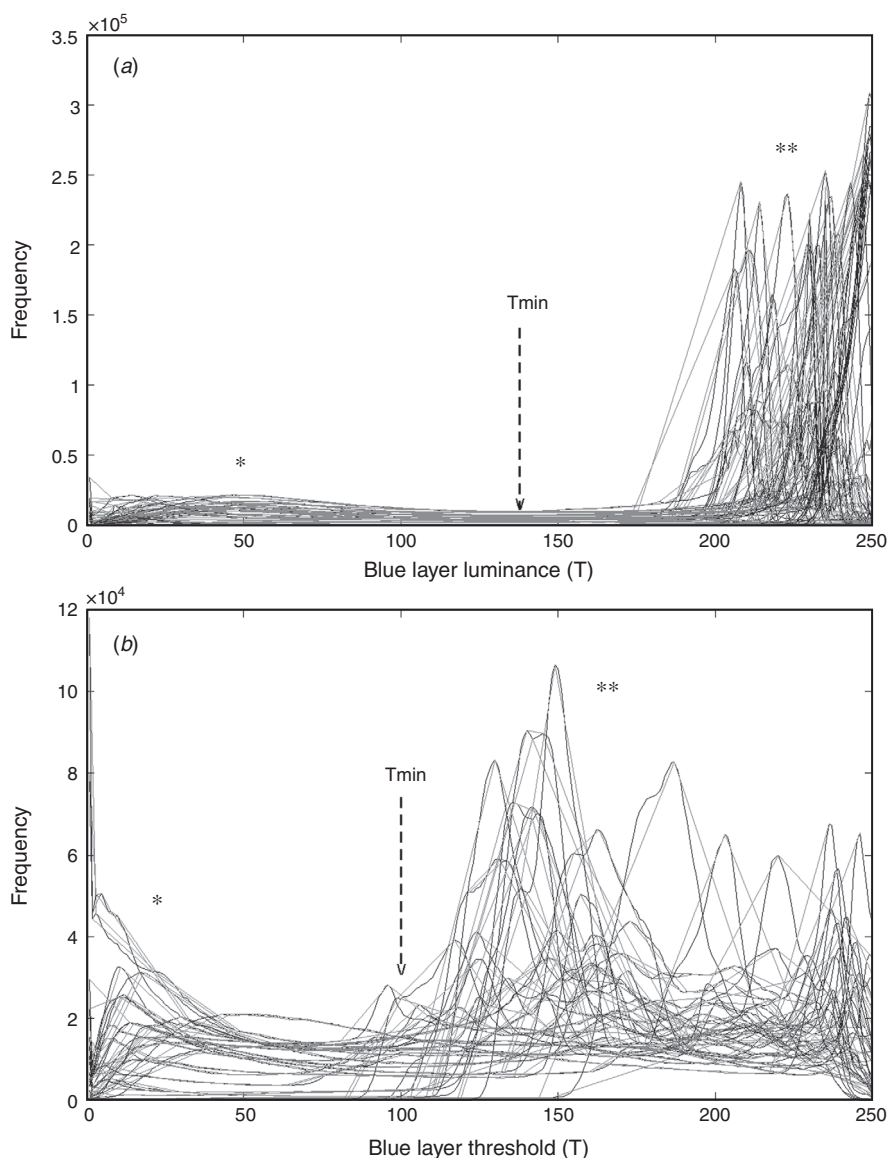


**Fig. 7.** (a) Histograms of blue layer luminance distributions for 50 images obtained on clear days and (b) 30 images on patchy cloudy days to perform a sensitivity analysis of LAI<sub>M</sub> to T. A baseline luminance threshold (Tmin) is selected at minimum frequency between the peaks corresponding to sky (\*) and foliage (\*\*).

available to interested researchers with access to MATLAB, the Image Analysis Toolbox and Image Acquisition Toolbox. An.exe version of the software will be available in the future as a graphic user interface (GUI) after compiling the script to run the program independently of MATLAB in any personal computer.

#### LAI estimations using MODIS LAI

The regression  $\text{MODIS LAI} = 0.9591 \text{ LAI}_D - 0.2371 (R^2 = 0.89)$  describes the relationship between  $\text{LAI}_D$  and MODIS LAI for the eight sites examined (Fig. 4, closed circles). For most of the sites, MODIS LAI tended to slightly overestimate  $\text{LAI}_M$ . We attribute this result to the fact that MODIS LAI includes the LAI of the understorey but  $\text{LAI}_D$  does not. Although we used dry season MODIS LAI in the comparison, an averaged contribution of the order of 15% understorey to total site LAI for dry season images is to be expected (unpublished observations). When including the  $\Omega(0)$  in the  $\text{LAI}_D$  calculation, the linear regression describing the  $\text{LAI}_e$  v. MODIS LAI relationship improved (MODIS LAI =  $1.0296 \text{ LAI}_e + 0.3468; R^2 = 0.91$ ). Despite this, MODIS LAI was consistently larger than  $\text{LAI}_e$  (Fig. 4, open triangles). In this case, a total mean understorey contribution of 17% was observed, which did not significantly change from uncorrected  $\text{LAI}_D$  measurements. Another source of discrepancy between  $\text{LAI}_D$  and MODIS LAI is the accuracy of collection 4 used in this study. Collection 5 has been released recently, which can achieve better agreement of retrieved and measured ground LAI. Digital imagery analysis and availability of foliage clumping estimates can provide a useful  $\text{LAI}_D$  comparison with other methods, such as MODIS LAI (collection 5), to examine the understorey contribution to total forest LAI. Consequently, understorey LAI contribution can easily be incorporated in  $\text{LAI}_D$  measurements when capturing images at 30 cm from the ground rather than 1.5 m, or at both heights for comparative purposes. If the MODIS LAI C5 is to become more universally applicable outside of evergreen woodland and forest, robust and efficient methods for estimating grass and understorey contribution need to be improved and automated. He *et al.* (2007) report that two conventional LAI instruments (LAI 2000 plant canopy analyser and AccupPAR Ceptometer), consistently underestimate grass LAI relative to destructive measurement.

Seasonal differences in LAI can be clearly seen using MODIS data and a GIS program (IDRISI; Clark Laboratories) for summer (Fig. 6a; 17 January 2006) and spring (Fig. 6b; 30 September 2006). A higher MODIS LAI is shown in January for woodland locations around NSW close to Sydney (MODIS LAI = up to 4.5) (Fig. 6a). A lower value for MODIS LAI (up to 2.5) was reached in spring for most of the woodland area seen in Fig. 6b.

#### Sensitivity analysis of $\text{LAI}_M$ to $T$

A sensitivity analysis on  $\text{LAI}_M$  to  $T$  was performed to assess the error associated to misdetection of a suitable  $T_{\min}$  for global  $\text{LAI}_M$  analysis. Fig. 7 shows the blue layer histograms corresponding to 50 images obtained in clear day conditions (Fig. 7a) and 30 images in cloudy day conditions (Fig. 7b). Frequency distribution of the blue layer luminance was more uniform for clear days rather than cloudy days. Therefore, it is easier to select a suitable common  $T$  ( $T_{\min} = 130$ ; Fig. 7a) for

clear days. This common  $T$  selection allows complete automation of image analysis using the script developed. On the contrary, selecting a common  $T$  for cloudy days is more complicated and could lead to over or underestimation of  $\text{LAI}_M$  for individual images ( $T_{\min} = 100$ ) (Fig. 7b). Therefore, the semiautomatic method is recommended for images taken under patchy cloudy day conditions (see earlier). Figure 8 and Table 2 show results of the sensitivity test for clear and patchy cloudy day conditions. The sensitivity of  $\text{LAI}_M$  to  $T$  increases with the magnitude of error of selection of  $T$  ( $\delta T$ ) for both clear and patchy cloudy day images. Dispersion of data points was smaller

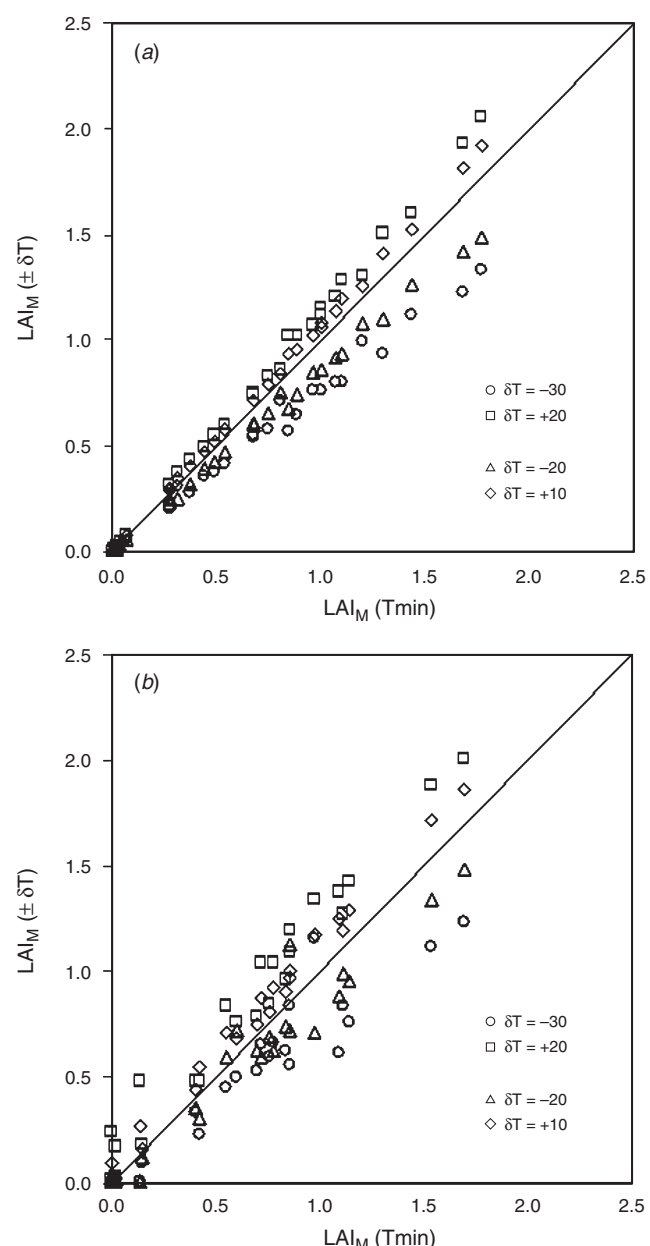


**Fig. 8.** Sensitivity analysis of  $\text{LAI}_M$  to  $T$  conducted for (a) 50 images on clear days, and (b) 30 images on patchy cloudy days. The magnitude of error used were  $\delta T = -30; +20; -20$  and  $+10$ . The baseline used was  $T_{\min}$ .

**Table 3. Results of sensitivity test on LAI<sub>M</sub> to T**

The analysis is done comparing a common T<sub>min</sub> selected as baseline for all images obtained in clear days ( $t=130$ ; LAI<sub>M</sub>=0.49) and for patchy cloudy day images ( $t=100$ ; LAI<sub>M</sub>=0.59). T<sub>min</sub> corresponded to luminosity value with minimal frequency for the majority of images

Parameters		$r^2$	b	RMSE	SEE	LAI <sub>M</sub>
<i>Clear days (n = 50); LAI<sub>D</sub> = 0.49</i>						
T <sub>min</sub> (baseline) v. T ± δ	δ <sub>t</sub> =-30	1.00	0.75	0.03	0.037	0.38
	δ <sub>t</sub> =+20	1.00	1.14	0.02	0.019	0.56
	δ <sub>t</sub> =-20	1.00	0.86	0.02	0.013	0.42
	δ <sub>t</sub> =+10	1.00	1.07	0.01	0.004	0.53
<i>Cloudy days (n = 30); LAI<sub>D</sub> = 0.68</i>						
T <sub>min</sub> (baseline) v. T ± δ	δ <sub>t</sub> =-30	0.92	0.76	0.11	0.313	0.46
	δ <sub>t</sub> =+20	0.97	1.17	0.01	0.236	0.27
	δ <sub>t</sub> =-20	0.95	0.89	0.10	0.244	0.52
	δ <sub>t</sub> =+10	1.00	1.03	0.04	0.047	0.68

for clear days (Fig. 8a) compared with patchy cloudy days (Fig. 7b). In the later case, the magnitude of error in selecting a suitable common T is considerably higher compared with clear days, as can be seen by comparing the correlation coefficients ( $r^2$ ), root mean square error (RMSE) and the standard error of estimates (SEE) (Table 3). Average RMSE=0.02; SEE=0.018 and  $r^2=1.0$  were found for clear days, and RMSE=0.07; SEE=0.21 and  $r^2=0.96$  for cloudy days. There was no considerable change in the slopes (b) obtained in the sensitivity test for cloudy days compared with clear days, since b is more dependant of the levels of misdetection errors selected for the sensitivity analysis ( $\delta t$ ). A maximum error of 4% from T<sub>min</sub> selected ( $\delta t=+10$ ) (considering a maximum value of  $t=250$ ; Fig. 3) did not affect considerably LAI<sub>M</sub>=0.53 compared with LAI<sub>D</sub>=0.49, for clear days (Table 3). The T<sub>min</sub> selected for clear days resulted in LAI<sub>M</sub>=0.49 compared with LAI<sub>D</sub>=0.49. Therefore, it is easier to select a suitable T for these conditions. For patchy cloudy day conditions, a common T value and considering  $\delta t=4\%$  error results between LAI<sub>M</sub> and LAI<sub>D</sub> where similar (LAI<sub>M</sub>=0.68; s.d.=0.55 compared with LAI<sub>D</sub>=0.68; s.d.=0.33). This means that a suitable T corresponded to T<sub>min</sub>=110 for these conditions. However, the correlation from individual pictures was lower ( $r^2=0.78$ ; b=0.84; RMSE=0.34; SEE=0.37) than results using the semi automated method for individual images: LAI<sub>M</sub>=0.68; s.d.=0.40; LAI<sub>D</sub>=0.68; s.d.=0.33 ( $r^2=0.95$ ; b=0.91; RMSE=0.12; SEE=0.62). These results showed that images including patchy clouds (Fig. 1) require the semi automated procedure for more accurate LAI<sub>M</sub> estimations on individual images. On the contrary, for clear days or completely overcast days, a common selection of T from the blue layer histograms (Fig. 7a) may allow a maximum of 4% error in the selection of a suitable T value for fully automated analysis.

## Conclusions

We conclude that digital image acquisition, coupled with MATLAB image data analysis, provides a rapid, robust, cheap and simple method for determining the LAI of tree canopies. Furthermore, we conclude that for evergreen woodland, where seasonal understorey growth is limited due to seasonal or stochastic drought, the MODIS LAI product provides a useful

surrogate for LAI<sub>D</sub>. However, as the contribution of the understorey to total site LAI increases, this is increasingly untrue. Renewed efforts to improve estimates of understorey LAI, together with the results from the script developed, will improve the quality of input of LAI into functional structural plant models and validation for retrieved MODIS LAI (collection 5).

## Acknowledgements

We thank Chris Hunt from Agresearch, Grasslands in New Zealand for his technical support.

## References

- Arias D, Calvo-Alvarado J, Dohrenbusch A (2007) Calibration of LAI-2000 to estimate leaf area index (LAI) and assessment of its relationship with stand productivity in six native and introduced tree species in Costa Rica. *Forest Ecology and Management* **247**, 185–193. doi: 10.1016/j.foreco.2007.04.039
- Bréda NJJ (2003) Ground-based measurements of leaf area index: a review of methods, instruments and current controversies. *Journal of Experimental Botany* **54**, 2403–2417. doi: 10.1093/jxb/erg263
- Carlson TN, Ripley DA (1997) On the relation between NDVI, fractional vegetation cover, and leaf area index. *Remote Sensing of Environment* **62**, 241–252. doi: 10.1016/S0034-4257(97)00104-1
- Chason JW, Baldocchi DD, Huston MA (1991) A comparison of direct and indirect methods for estimating forest canopy leaf area. *Agricultural and Forest Meteorology* **57**, 107–128. doi: 10.1016/0168-1923(91)90081-Z
- Chen JM, Cihlar J (1995) Plant canopy gap-size analysis theory for improving optical measurements of leaf area index. *Applied Optics* **34**, 6211–6222.
- Cutini A, Matteucci G, Mugnozza GS (1998) Estimation of leaf area index with the Li-Cor LAI 2000 in deciduous forests. *Forest Ecology and Management* **105**, 55–65. doi: 10.1016/S0378-1127(97)00269-7
- De Reffye P, Houllier F, Blaise F, Barthelemy D, Dauzat J, Auclair D (1995) A model simulating above- and below-ground tree architecture with agroforestry applications. *Agroforestry Systems* **30**, 175–197. doi: 10.1007/BF00708920
- Ewert F (2004) Modelling plant responses to elevated CO<sub>2</sub>: how important is leaf area index? *Annals of Botany* **93**, 619–627. doi: 10.1093/aob/mch101
- Frazer GW, Fournier RA, Trofymow JA, Hall RJ (2001) A comparison of digital and film fisheye photography for analysis of forest canopy structure and gap light transmission. *Agricultural and Forest Meteorology* **109**, 249–263. doi: 10.1016/S0168-1923(01)00274-X
- He YH, Guo XL, Wilmhurst JF (2007) Comparison of different methods for measuring leaf area index in a mixed grassland. *Canadian Journal of Plant Science* **87**, 803–813.

- Huang D, Knyazikhin Y, Wang W, Deering DW, Stenberg P, Shabanov N, Tan B, Myneni RB (2008) Stochastic transport theory for investigating the three-dimensional canopy structure from space measurements. *Remote Sensing of Environment* **112**, 35–50. doi: 10.1016/j.rse.2006.05.026
- Johnson LF (2003) Temporal stability of an NDVI-LAI relationship in a Napa Valley vineyard. *Australian Journal of Grape and Wine Research* **9**, 96–101. doi: 10.1111/j.1755-0238.2003.tb00258.x
- Knyazikhin Y, Martonchik JV, Myneni RB, Diner DJ, Running SW (1998) Synergistic algorithm for estimating vegetation canopy leaf area index and fraction of absorbed photosynthetically active radiation from MODIS and MISR data. *Journal of Geophysical Research – Atmospheres* **103**, 32257–32275. doi: 10.1029/98JD02462
- Kucharik CJ, Norman JM, Murdock LM (1997) Characterising canopy nonrandomness with a multiband vegetation imager (MVI). *Journal of Geophysical Research* **102**, 455–429. doi: 10.1029/97JD01175
- Lu L, Shuttleworth WJ (2002) Incorporating NDVI-Derived LAI into the climate version of RAMS and its impact on regional climate. *Journal of Hydrometeorology* **3**, 347–362. doi: 10.1175/1525-7541(2002)003<0347:INDLIT>2.0.CO;2
- Macfarlane C, Coote M, White DA, Adams MA (2000) Photographic exposure affects indirect estimation of leaf area in plantations of *Eucalyptus globulus* Labill. *Agricultural and Forest Meteorology* **100**, 155–168. doi: 10.1016/S0168-1923(99)00139-2
- Macfarlane C, Arndt SK, Livesley SJ, Edgar AC, White DA, Adams MA, Eamus D (2007a) Estimation of leaf area index in eucalypt forest with vertical foliage, using cover and fullframe fisheye photography. *Forest Ecology and Management* **242**, 756–763. doi: 10.1016/j.foreco.2007.02.021
- Macfarlane C, Hoffman M, Eamus D, Kerp N, Higginson S, McMurtrie R, Adams M (2007b) Estimation of leaf area index in eucalypt forest using digital photography. *Agricultural and Forest Meteorology* **143**, 176–188. doi: 10.1016/j.agrformet.2006.10.013
- Macfarlane C, Grigg A, Evangelista C (2007c) Estimating forest leaf area using cover and fullframe fisheye photography: thinking inside the circle. *Agricultural and Forest Meteorology* **146**, 1–12. doi: 10.1016/j.agrformet.2007.05.001
- Nemani R, Pierce L, Running S, Band L (1993) Forest ecosystem processes at the watershed scale: sensitivity to remotely-sensed leaf area index estimates. *International Journal of Remote Sensing* **14**, 2519–2534. doi: 10.1080/01431169308904290
- Peterson DL, Spanner MA, Running SW, Teuber KB (1987) Relationship of thematic mapper simulator data to leaf area index of temperate coniferous forests. *Remote Sensing of Environment* **22**, 323–341. doi: 10.1016/0034-4257(87)90087-3
- Tian Y, Woodcock CE, Wang Y, Privette JL, Shabanov NV et al. (2002) Multiscale analysis and validation of the MODIS LAI product: II. Sampling strategy. *Remote Sensing of Environment* **83**, 431–441. doi: 10.1016/S0034-4257(02)00058-5
- Villalobos FJ, Orgaz F, Mateos L (1995) Non-destructive measurement of leaf area in olive (*Olea europaea* L.) trees using a gap inversion method. *Agricultural and Forest Meteorology* **73**, 29–42. doi: 10.1016/0168-1923(94)02175-J
- Watson DJ (1947) Comparative physiological studies on the growth of field crops: I. Variation in net assimilation rate and leaf area between species and varieties, and within and between years. *Annals of Botany* **11**, 41–76.
- Whitley R, Zeppel M, Armstrong N, Macinnis-Ng C, Yunusa I, Eamus D (2008) A modified Jarvis-Stewart model for predicting stand-scale transpiration of an Australian native forest. *Plant and Soil* **305**, 35–47. doi: 10.1007/s11104-007-9399-x
- Zeppel MJB, Murray BR, Barton C, Eamus D (2004) Seasonal responses of xylem sap velocity to VPD and solar radiation during drought in a stand of native trees in temperate Australia. *Functional Plant Biology* **31**, 461–470. doi: 10.1071/FP03220
- Zeppel M, Macinnis-Ng CMO, Ford CR, Eamus D (2008) The response of sap flow to pulses of rain in a temperate Australian woodland. *Plant and Soil* **305**, 121–130. doi: 10.1007/s11104-007-9349-7

Manuscript received 5 March 2008, accepted 25 September 2008